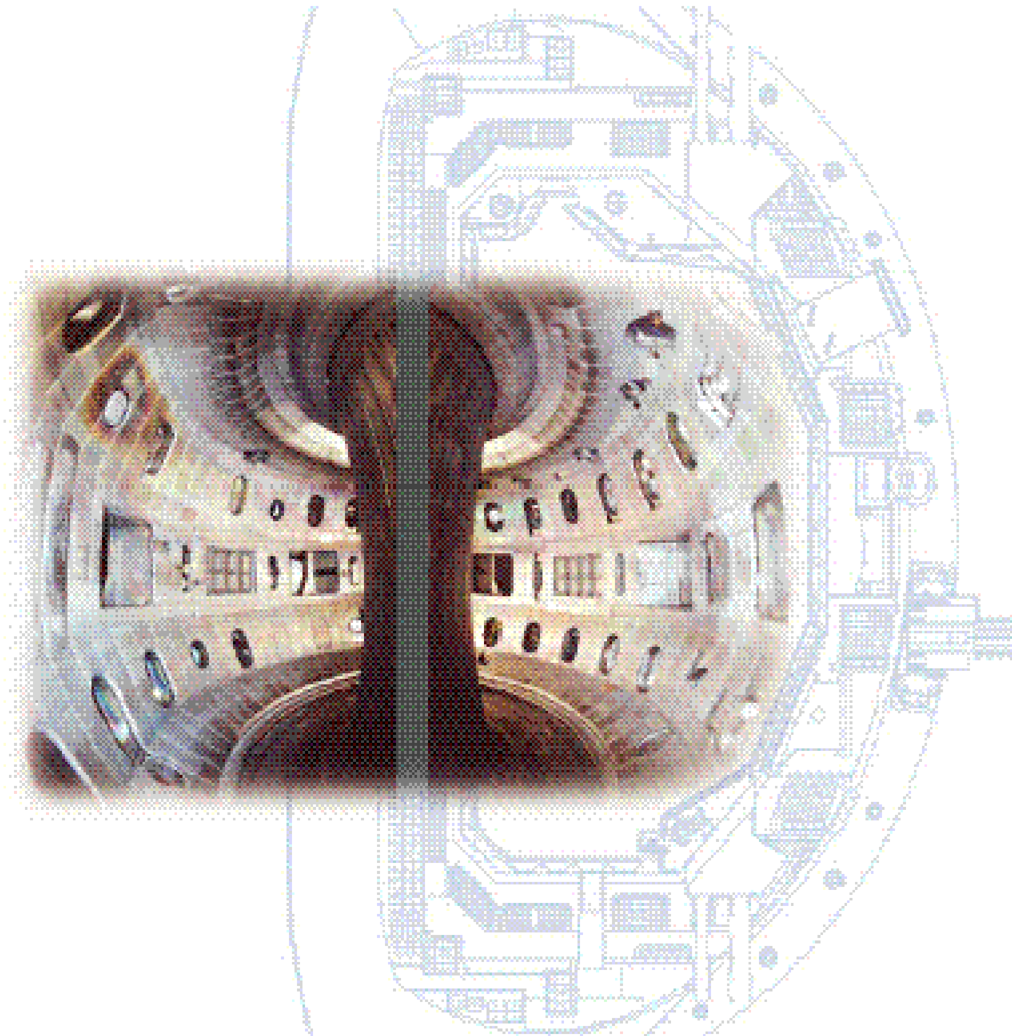

Structure, Stability and ELM Dynamics of the H-mode Pedestal in DIII-D

M.E. Fenstermacher (LLNL)
for the DIII-D Team

Presented at the
2004 IAEA Fusion Energy Conference,
Villamoura, Portugal,
November 1-6, 2004

Outline: This poster organized in 5 sections

- **Motivation**
  - Pedestal height determines H-mode performance and ELMs could limit divertor and main wall lifetimes
- **Pedestal Structure and ρ_* scaling**
  - Similarity experiments show neutral penetration dominates in setting density pedestal width but not temperature pedestal width and lack of ρ_* scaling
- **Pedestal Stability**
  - Linear peeling-ballooning in equilibrium constrained by measured edge current predicts ELM onset conditions
- **ELM Dynamics**
  - Measurements and initial non-linear simulations point to complex spatial and temporal structure of ELMs
- **Conclusions**

Motivation: Understanding and controlling the H-mode pedestal is a critical issue for future tokamaks (ITER)

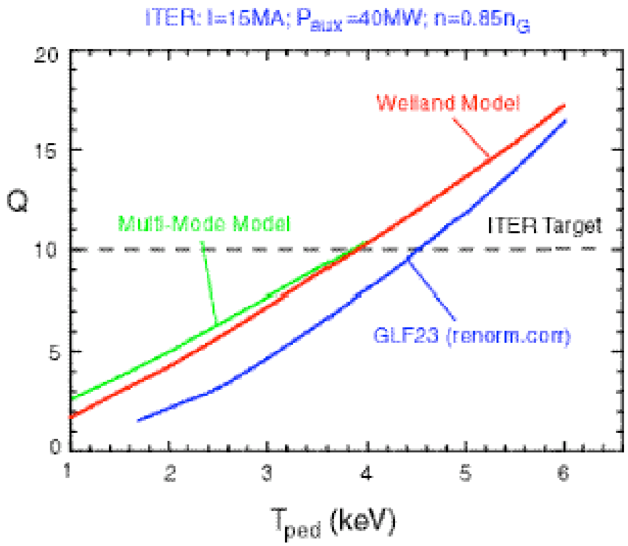

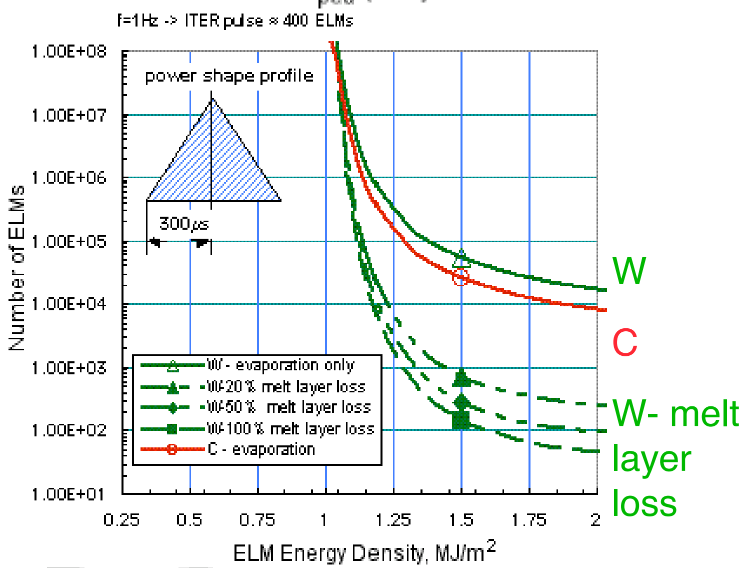

- **For stiff profiles, pedestal height determines energy confinement and overall performance - Q**
  - **The pedestal is the boundary condition for the core**
- **Type-I ELMs in ITER could potentially limit the divertor and first wall lifetime**
- **Multi-disciplinary work at DIII-D including transport, stability and boundary physics**
- **The goal of this research area is to:**
  - **Predict and control the edge pedestal width / height and ELM particle and energy losses**

Summary I: Pedestal similarity experiments in DIII-D and JET show neutrals dominate in setting density pedestal width

Osborne APS03

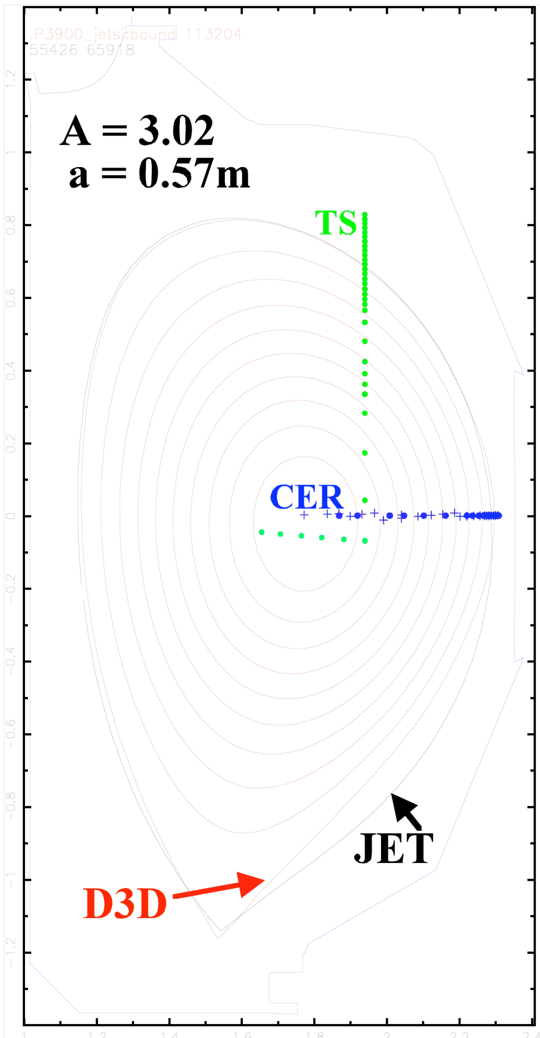

- **Similarity experiments requested by pedestal ITPA**
  - **Matched shapes in DIII-D and JET are optimized for pedestal diagnostics.**
  - **Dimensionless parameters matched at the top of the pedestal**

$$\beta \sim \frac{nT}{B^2}, \quad \rho_* \sim \frac{T^{1/2}}{aB}, \quad \nu_* \sim \frac{an}{T^2} A^{5/2} q, \quad q \sim \frac{aB}{AI}$$

  - **Scan of ρ* also done by varying B_T**
- **Neutral penetration physics dominates in setting the density width**
- **Plasma physics dominates in setting the Te width (transport barrier)**
- **Transport barrier not a strong function of ρ* for fixed (β, ν*, q)**
- **ELM size decreased as ρ * decreased for constant (β, ν*, q) but neutral penetration also playing a role**

DIII-D EFDA JET

Summary II: ELM onset predicted by linear peeling-ballooning model constrained by measured j_{edge}

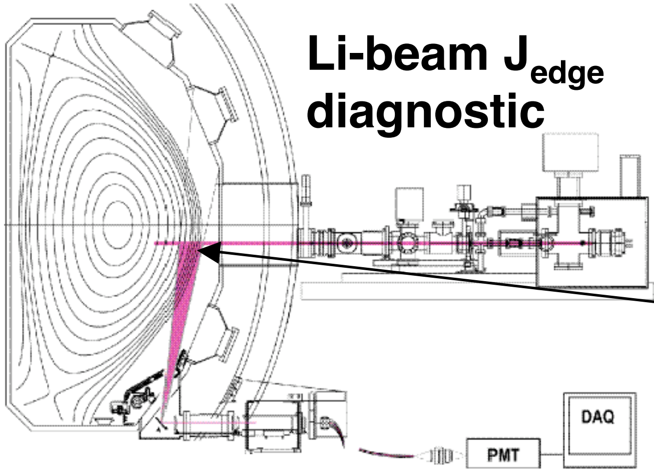

Li-beam J_{edge} diagnostic

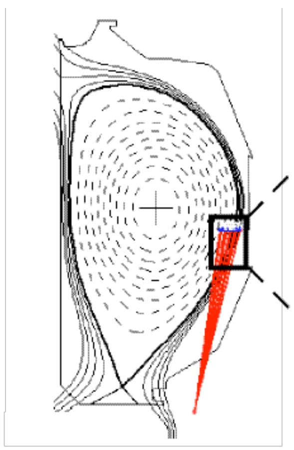

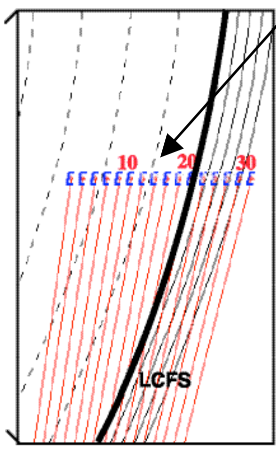

Geometry of view chords

- **Pedestal stability physics investigated in dedicated experiments with new diagnostics**
  - Pedestal current density by polarimetry of Li-beam
    - comparison with theory of j_{bs}
    - Constraint on edge stability calculation
  - Fast gated intensified images of ELM structure
- **Linear peeling-ballooning instability calculation in equilibrium constrained by edge current data shows unstable intermediate-n modes**
  - Fast camera images show similar mode structure

Summary III ELM dynamics in the pedestal and SOL show evidence of complex spatial and temporal structure

3D rendering of P-B mode structure

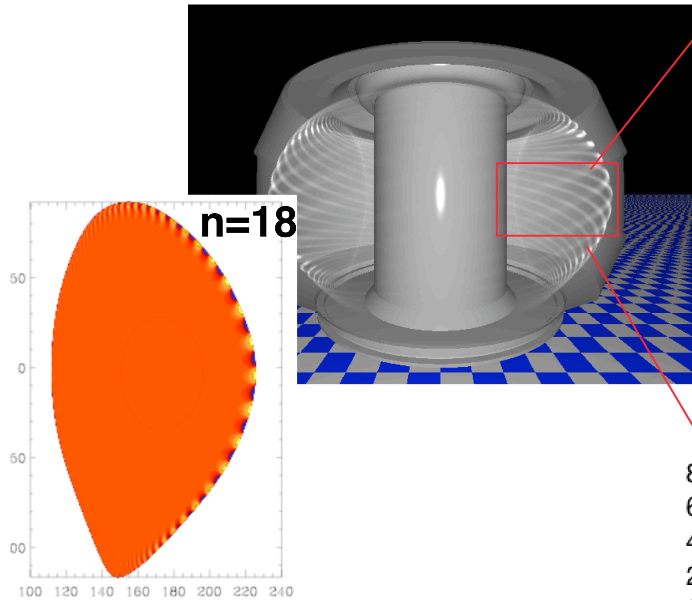

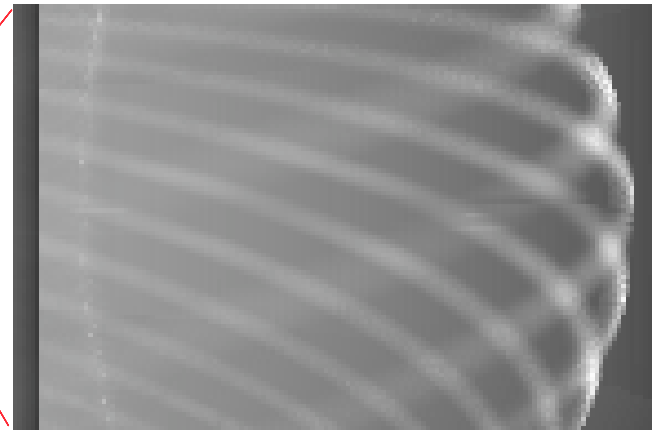

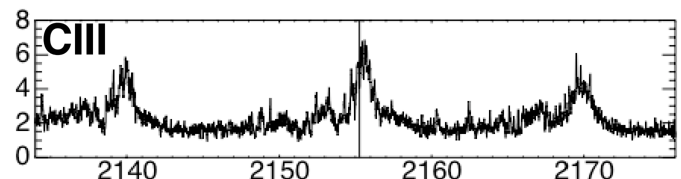

Camera view in reflected light

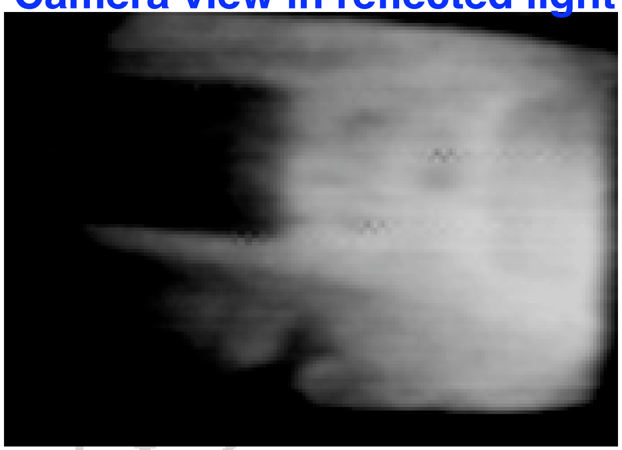

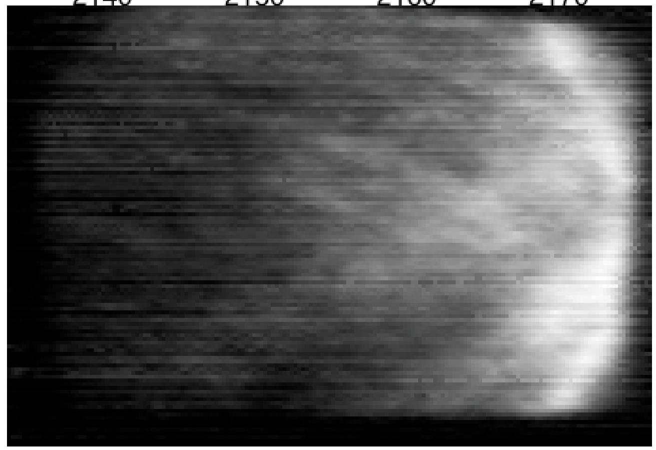

- Structure of linear P-B ELM instability seen in CIII image data during ELM
- Most unstable modes from ELITE linear P-B instability are 18 ≤ n ≤ 21
- CIII emission structure suggests n ~ 17

Pedestal Profiles and Similarity Expts

Dimensionless parameter match in different size tokamaks tests whether neutral source or plasma physics controls ETB width

Osborne APS03

- **Matching the dimensionless parameters**

$$\beta \sim \frac{nT}{B^2}, \quad \rho_* \sim \frac{T^{1/2}}{aB}, \quad \nu_* \sim \frac{an}{T^2} A^{5/2} q, \quad q \sim \frac{aB}{AI}$$

$$\Rightarrow n \sim a^{-2}, \quad T \sim A^{5/4} a^{-1/2}, \quad B \sim A^{5/8} a^{-5/4}, \quad I \sim A^{-3/8} a^{-1/4}$$

- **If plasma physics controls the ETB width, normalized width should not vary with machine size**

$$\hat{\Delta}_T = \Delta_T / a \approx const$$

- **If neutrals control the edge density profile and ETB width, normalized width should vary as minor radius for same poloidal distribution of the neutral source**

$$\hat{\Delta}_T \sim \hat{\Delta}_n = \frac{\Delta_n}{a} \sim \frac{1}{anE^*} \sim a / E^*$$

where E^* is the flux expansion averaged over the poloidal distribution of the neutral source.

DIII-D NATIONAL FUSION FACILITY

Neutral penetration model predicts density pedestal width; temperature pedestal width scales with minor radius

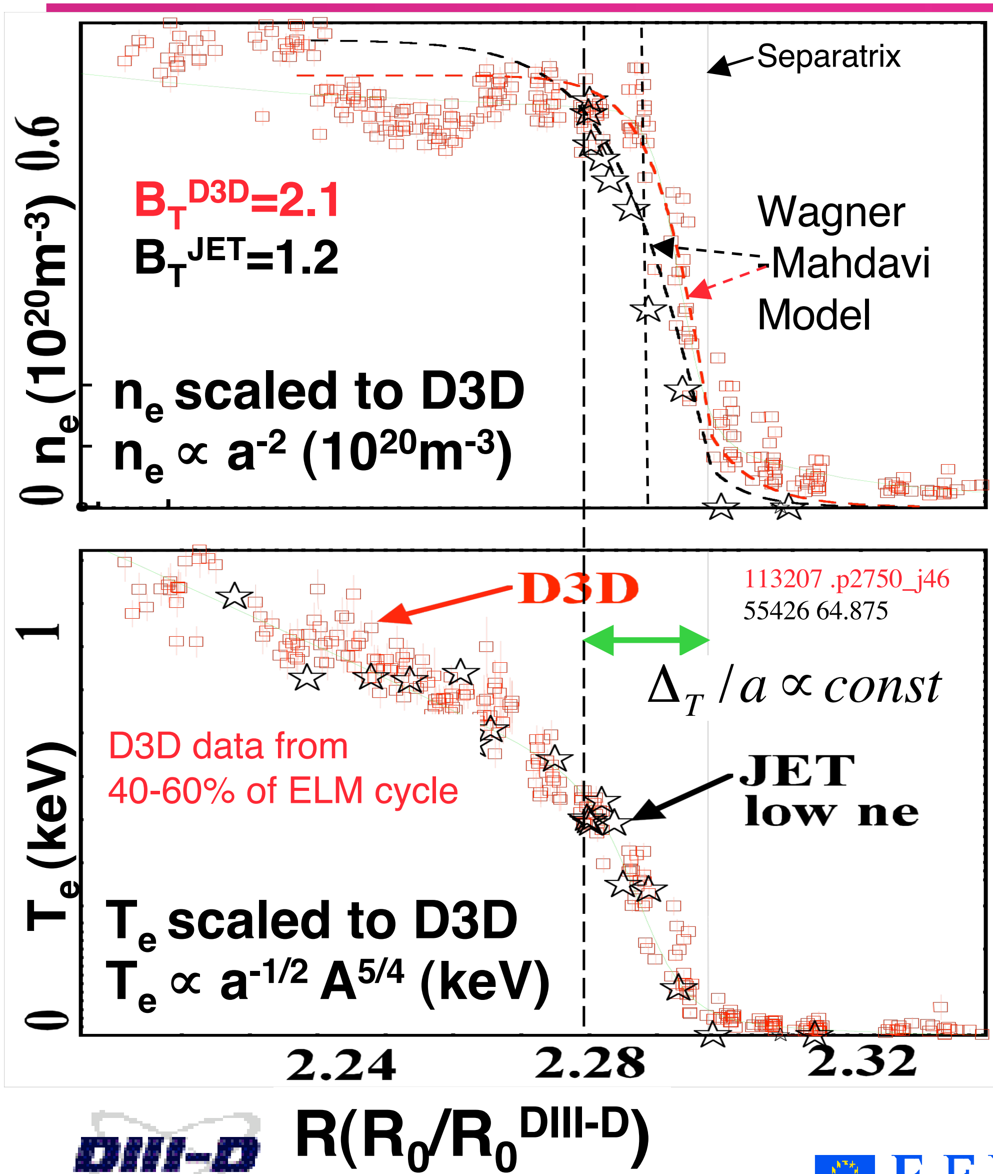

Osborne APS03

- **Wagner-Mahdavi model reproduces Δ_{ne}**
- **Model reproduces observations:**
  - **DIII-D : top of n_e pedestal farther out than top of T_e pedestal**
  - **JET: top of n_e pedestal farther in than in DIII-D**
- **$\Delta_{Te} \propto$ a so not controlled by neutral penetration**
- **Scaling of Δ_{Te} favorable for ITER**

Structure of the edge density profile is consistent with Wagner-Mahdavi neutral source model

Osborne APS03

- **Englehardt-Wagner model[1] extended by Mahdavi[2] to include poloidal variation in neutral source and Franck-Condon neutrals**

$\nabla \cdot (D_{CORE} \nabla n_e - n_e V_{POL}) = -n_0 n_e S_i$: Diffusion balances ionization

$\nabla \cdot (n_0 V_0) = -n_0 n_e S_i$: Neutral flux reduced by ionization

In scrape-off layer $(\xi \geq 0)$, $n_e(\xi) = n_{sep} \exp[-\xi / \sqrt{D\tau_{\|}}]$

In the core $(\xi \leq 0)$,

$$n_e(\xi) = n_{ped} \tanh\left[C - \frac{S_i E^*}{2V_{0X}} n_{ped}\, \xi\right]$$

where $C \equiv 0.5 \sinh^{-1}(U)$, $U \equiv \sqrt{D_{SOL}\tau_{\|}} \frac{S_i}{V_{0X}} \frac{D_{CORE}}{D_{SOL}} E^* n_{ped}$,

and $\tau_{\|}$ is particle confinement time in SOL, $\xi = 1 - \rho$, and

E^* is the flux expansion weighted by the neutral particle source

For $U \leq 1$, $n_{ped} / n_{sep} \propto 2/U \Rightarrow$

$$n_{ped}^2 \propto n_{sep} / E^*$$

$$\Delta_{ne} \propto 1/(E^* n_{ped})$$

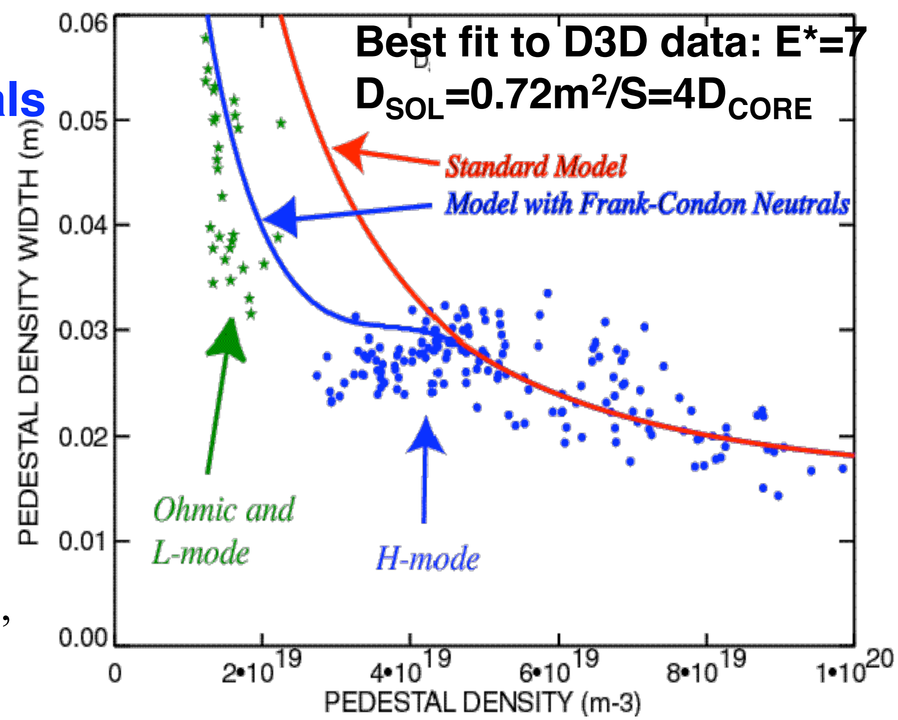

- **At high n_e neutrals cross separatrix as CX with local ion thermal velocity**
- **At low n_e neutrals are at Franck-Condon velocity**

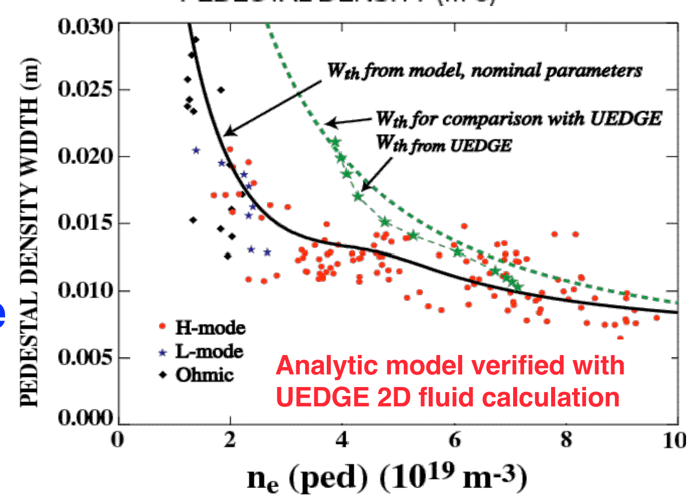

Analytic model verified with UEDGE 2D fluid calculation

DIII-D

[1]W. Engelhardt, W. Fenenberg, J. Nucl. Mater. **76-77** (1978) 518.
[2]M.A. Mahdavi et al., Plasma Phys. **10** (2003) 3988.

Neutral penetration model predicts narrowing of density pedestal width at high density; Δ_{Te}/a still constant

JET / DIII-D Similarity Experiment

Osborne APS03

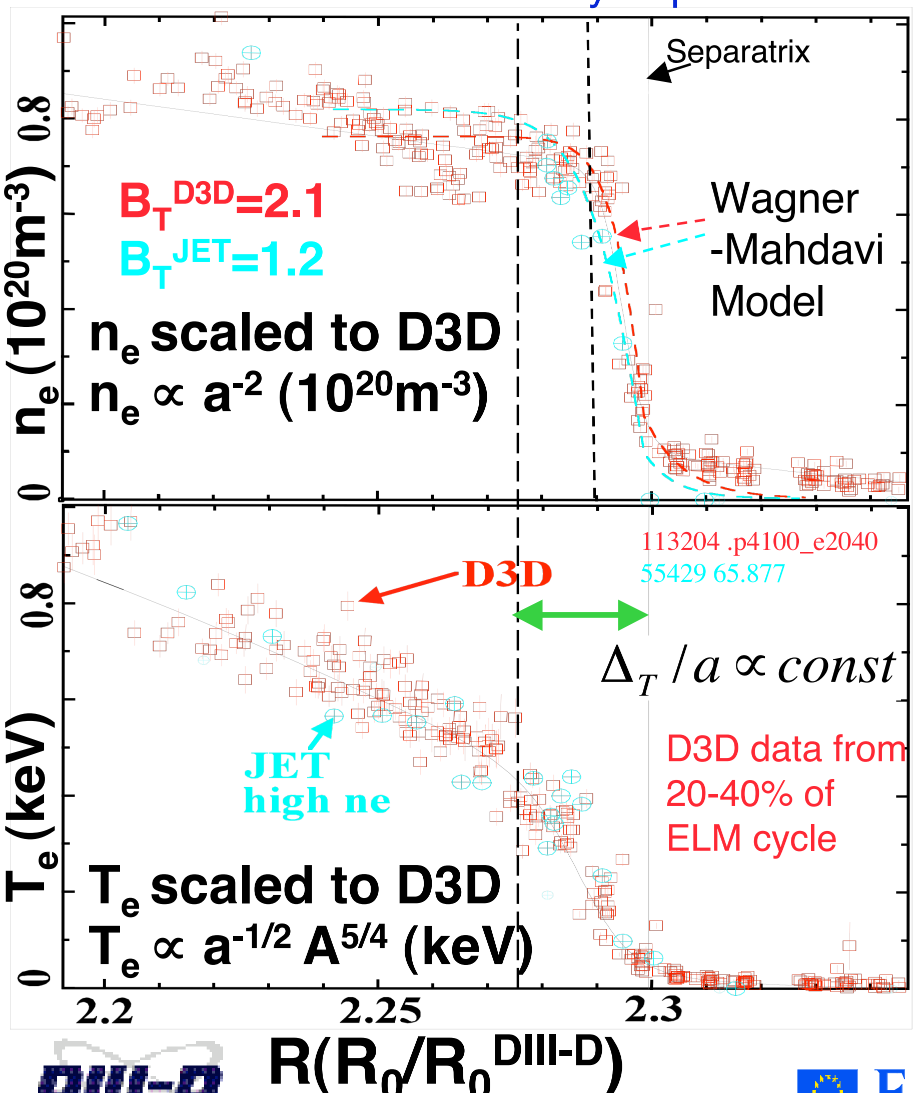

- **Wagner-Mahdavi model reproduces smaller Δ_{ne} at higher n_e**
- **Model predicts observation that $\Delta_{ne} \propto 1 / n_e^{ped}$**
- **$\Delta_{Te} \propto a$ for both low and high n_e discharges**
- **Neutral physics does not set transport barrier width**

ρ^* Scaling and Similarity Expts

Variation of B_T used to give scan in ρ_* with other dimensionless variables fixed

Osborne APS03

- **Maintaining β and ν_* fixed as B is varied at fixed q requires**

$$n \sim A^{-5/6} a^{-1/3} B^{4/3}, \quad T \sim A^{5/6} a^{1/3} B^{2/3}, \quad I \sim A^{-1} a B$$

- **Then ρ_* varies as**

$$\rho_* \sim A^{5/12} a^{-5/6} B^{-2/3}$$

- **Comparing a 1.0T discharge in DIII-D with a 2.7T case in JET would give a factor of 3.4 variation in ρ_***
- **Neutral penetration increases with ρ_***

$$\hat{\Delta}_n \sim a\, \rho_*^2 / E^*$$

Time averaged temperature pedestal width does not show a strong empirical scaling with ρ_*

Osborne APS03

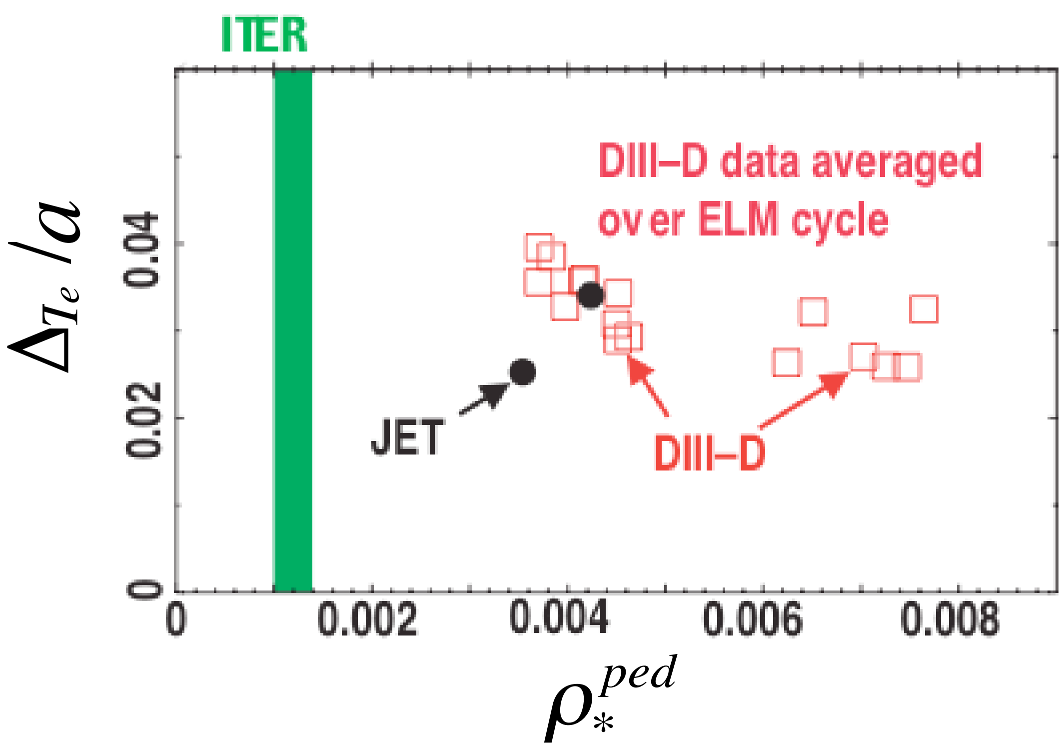

- **No strong dependence of Δ_T / a with ρ_* for DIII-D data alone**
- **$\Delta_{ne} \sim (\rho_*)^2$ seen in experiments consistent with Wagner-Mahdavi prediction for similarity experiments**

ELM energy loss scales with ρ* consistent with changing P/B mode width but neutral penetration also playing a role

Osborne APS03

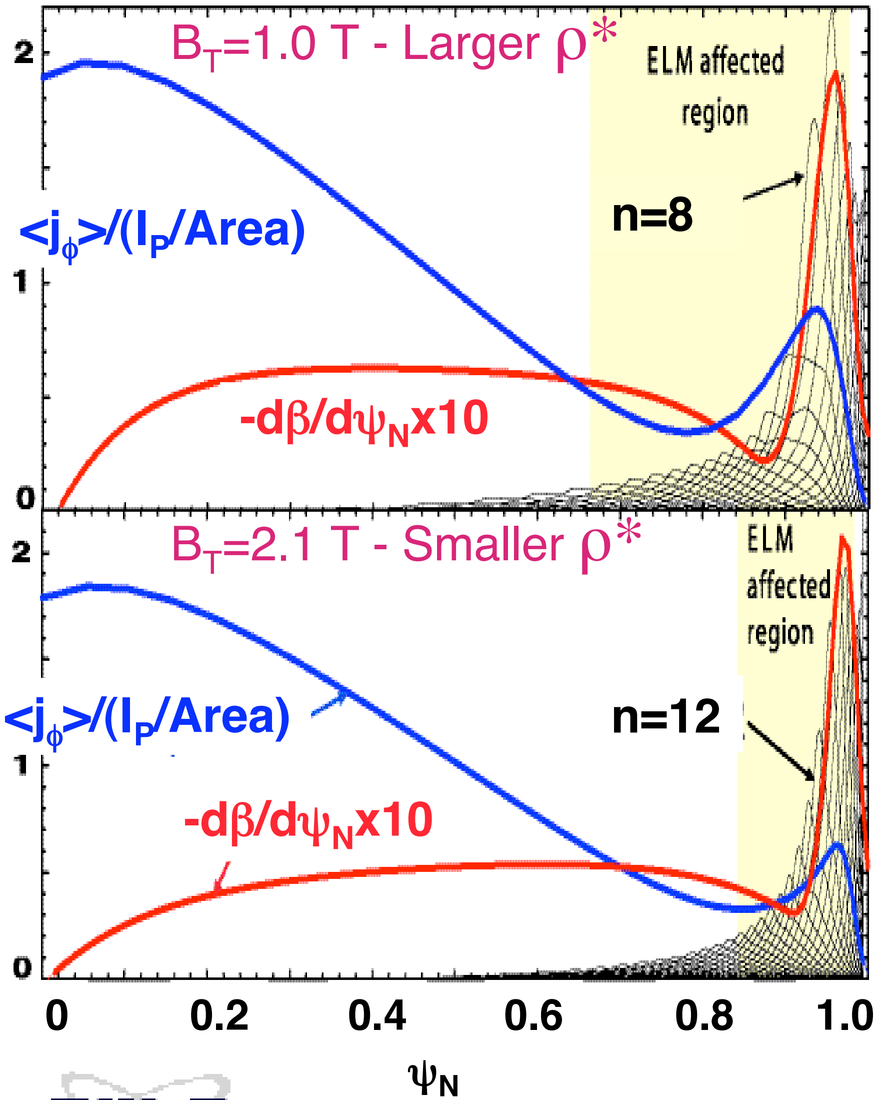

- **Trends favorable for ITER as ρ* decreased at fixed (β, ν_*, q):**
  - **ELM energy loss, $\Delta W_{ELM} / W_{ped}$ smaller and f_{ELM} larger**
  - **ELM affected region smaller**
  - **P/B modes had smaller radial extent**
  - **Duration of ELM magnetic fluctuations less and amplitude smaller**
  - **Pedestal β just before the ELM reduced due to outward shift of $n_e(r)$ from reduced neutral penetration**
- **Separablitiy of Δ_{ne} from Δ_{Te} may allow high pedestal and small ELMs**

ELM affected region larger at larger ρ* (DIII-D data)

Osborne APS03

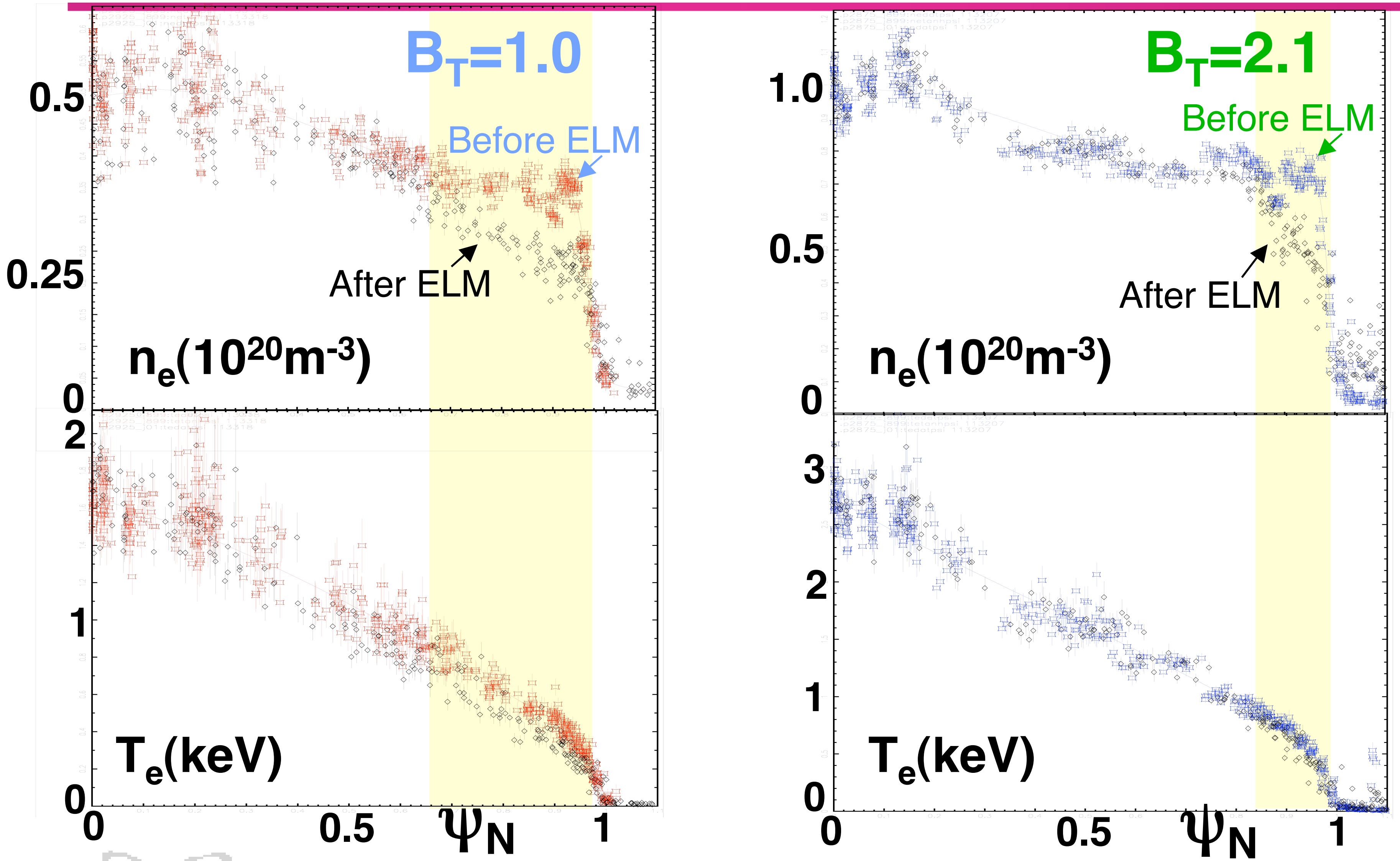

Neutral penetration playing a role in reduction of β_{PED} just before ELM and ELM size at small ρ_*

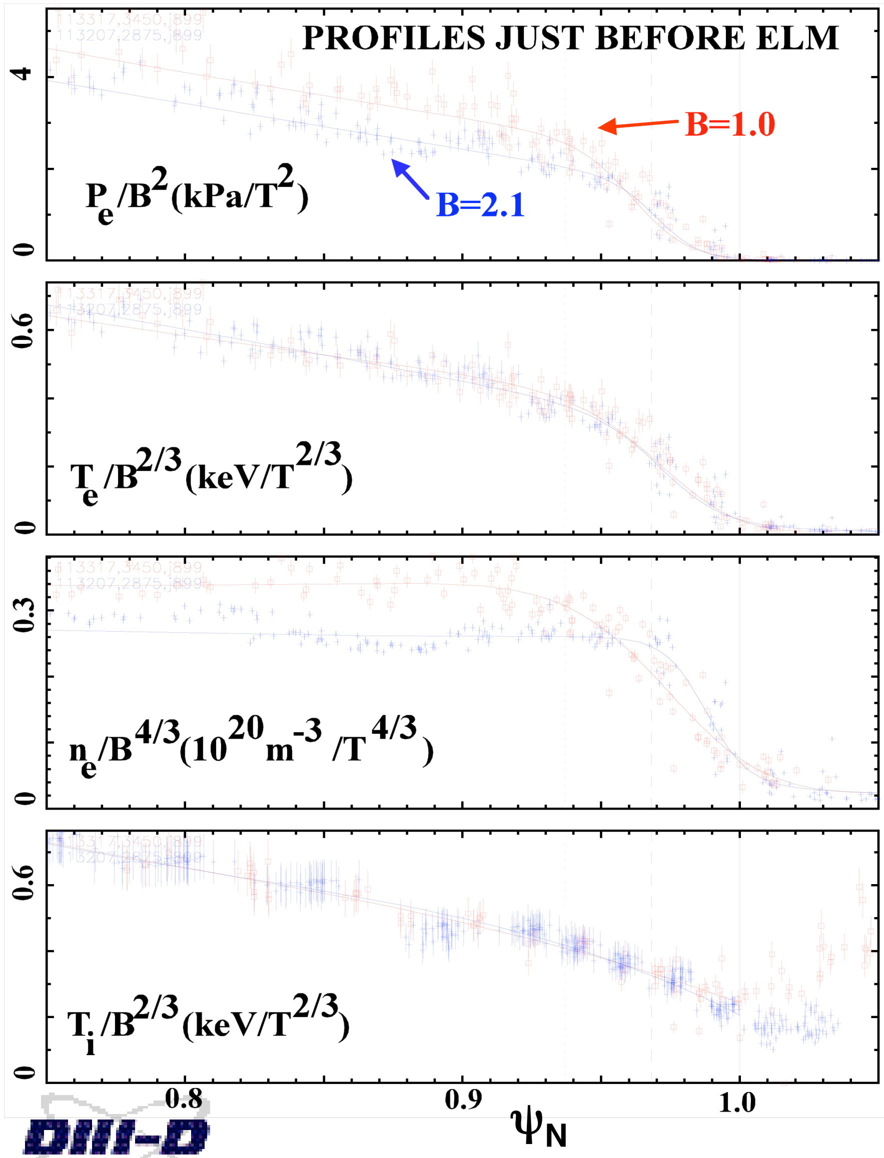

Osborne APS03

- Small ρ_* (high B) corresponds to higher n at fixed (β, ν_*, q)
- Outward shift of n_e profile from reduced neutral penetration at small ρ_*
- High p' region shifted outward and β_{PED} reduced at ELM crash.

Pedestal Stability and ELM Onset

Polarimetry of a Li-beam used to measure magnetic field pitch angle at plasma edge

Thomas, Leonard EPS 2004

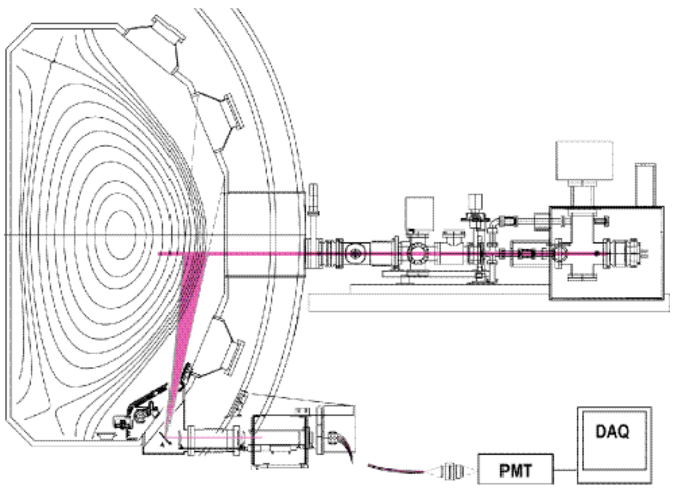

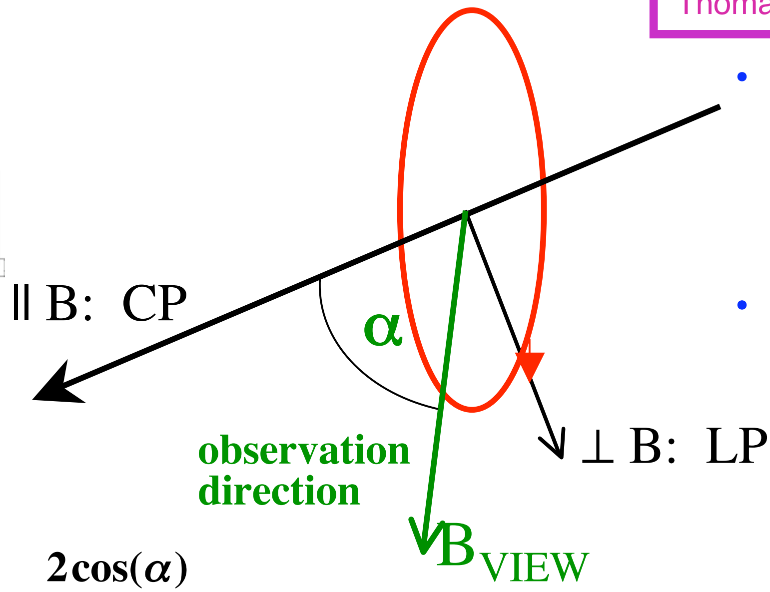

- **Select the σ– line with narrowband filter.**
- **Measure ratio of circular to linear polarization using dynamic polarimetry**

$$\text{Ratio}\left\{\frac{CP}{LP}\right\} = \frac{2\cos(\alpha)}{\sin^2(\alpha)}$$

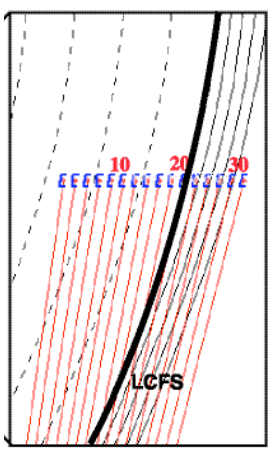

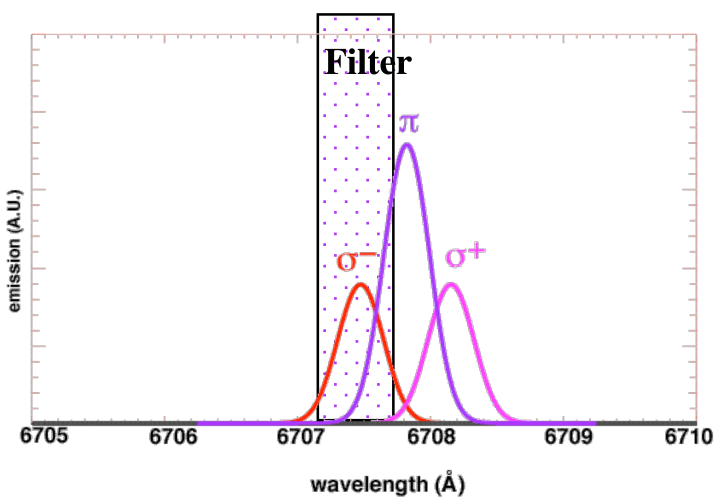

Then

B_{VIEW} (R,z)= |B| cos (α)

1) use as EFIT constraint

2) solve directly using

$$\mu_0 j_{TOR} = \frac{\partial B_R}{\partial z} - \frac{\partial B_z}{\partial R}$$

Ampere's Law approach - 1

Thomas, Leonard EPS 2004

- The spatial calibration defines the R, z location for each of the viewchords (red lines) as well as the view inclination angle θ_V -

$$B_{VIEW} = B_Z \cos\theta_V + B_R \sin\theta_V$$

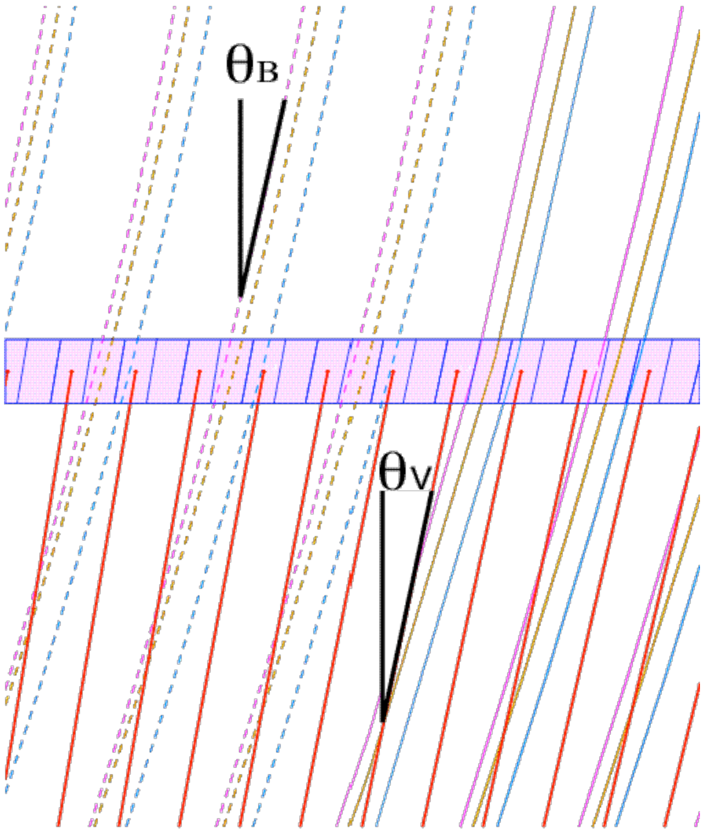

- Or, using the magnetic inclination angle θ_B ($\tan\theta_B = B_R/B_Z$)

$$B_{VIEW} = B_Z(\cos\theta_V + \sin\theta_V \tan\theta_B)$$

- ADVANTAGE: $\tan\theta_B$ is an insensitive function of the exact current distribution

=> can evaluate using any reasonable reconstruction (dotted lines).

Ampere's Law approach - 2

Thomas, Leonard EPS 2004

Then Ampere's law

$$\mu_0 j_{TOR} = \frac{\partial B_R}{\partial z} - \frac{\partial B_z}{\partial R}$$

may be written

$$\mu_0 j_{TOR} = \frac{\partial B_z}{\partial z} \tan\theta_B + B_z \frac{\partial \tan\theta_B}{\partial z} - \frac{\partial B_z}{\partial R}$$

and, from the definition of poloidal flux function in toroidal geometry

$$B_R = -\frac{1}{R}\frac{\partial \varphi}{\partial z}, \qquad B_z = \frac{1}{R}\frac{\partial \varphi}{\partial R}$$

we can take the appropriate partials to get

$$\frac{\partial B_z}{\partial z} = -\frac{1}{R}\frac{\partial}{\partial R}(RB_R) = -\frac{B_R}{R} - \frac{\partial B_R}{\partial R}$$

Ampere’s Law approach - 3

Or, again using the definition of $\tan\theta_B$

Thomas, Leonard EPS 2004

$$\frac{\partial B_z}{\partial z} = - B_z \frac{\tan\theta_B}{R} - \frac{\partial B_z}{\partial R}\tan\theta_B - B_z \frac{\partial \tan\theta_B}{\partial R}$$

And Ampere’s law may be written

$$\mu_0 j_{TOR} = B_z\left(\frac{\partial \tan\theta_B}{\partial z} - \frac{\tan^2\theta_B}{R} - \tan\theta_B \frac{\partial \tan\theta_B}{\partial R} \right) - \frac{\partial B_z}{\partial R}\left(1 + \tan^2\theta_B\right)$$

Finally, substituting for B_z with B_{VIEW} yields

$$\mu_0 j_{TOR} = B_{VIEW} \frac{\left[\frac{\partial \cos\theta_V}{\partial R} + \frac{\partial \sin\theta_V}{\partial R}\tan\theta_B + \sin\theta_V \frac{\partial \tan\theta_B}{\partial R} \right]\left[1 + \tan^2\theta_B\right]}{\left[\cos\theta_V + \sin\theta_V\left(\tan\theta_B\right)\right]^2}$$

$$+ B_{VIEW} \frac{\left[\frac{\partial \tan\theta_B}{\partial z} - \frac{\tan^2\theta_B}{R} - \tan\theta_B \frac{\partial \tan\theta_B}{\partial R} \right]}{\left[\cos\theta_V + \sin\theta_V\left(\tan\theta_B\right)\right]} - \frac{\partial B_{VIEW}}{\partial R}\left[\frac{1 + \tan^2\theta_B}{\cos\theta_V + \sin\theta_V\left(\tan\theta_B\right)} \right]$$

Agreement of bootstrap calculation and measured edge current increases confidence in equilibrium models

Thomas, Leonard PRL 2004

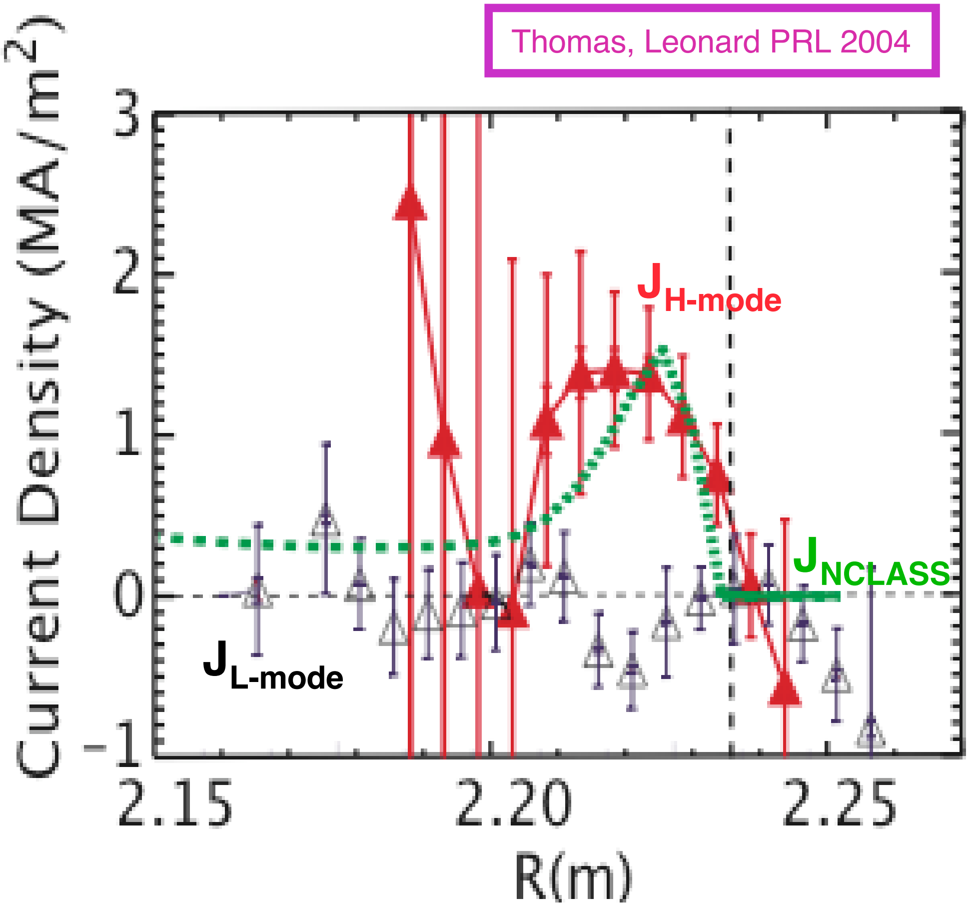

$$\mu_0 j_{TOR} = \frac{\partial B_R}{\partial z} - \frac{\partial B_z}{\partial R}$$

- Large $J_{H\text{-mode}}$ = 1.5 MA/m² measured in H-mode for the first time with Li-beam polarimetry diagnostic compared with negligible $J_{L\text{-mode}}$ in L-mode
  - Toroidal j_{edge} calculated directly from Ampere's law
- Magnitude of $J_{H\text{-mode}}$ agrees with calculation of $J_{NCLASS} = J_{BS} + J_{PS}$ from NCLASS code
  - EFIT constrained by plasma pressure profiles and NCLASS bootstrap current
- Provides increased confidence in equilibrium reconstructions with finite edge current

ELITE calculation on equilibrium constrained by measured j_{edge} shows instability at ELM onset

Thomas, Leonard EPS 2004

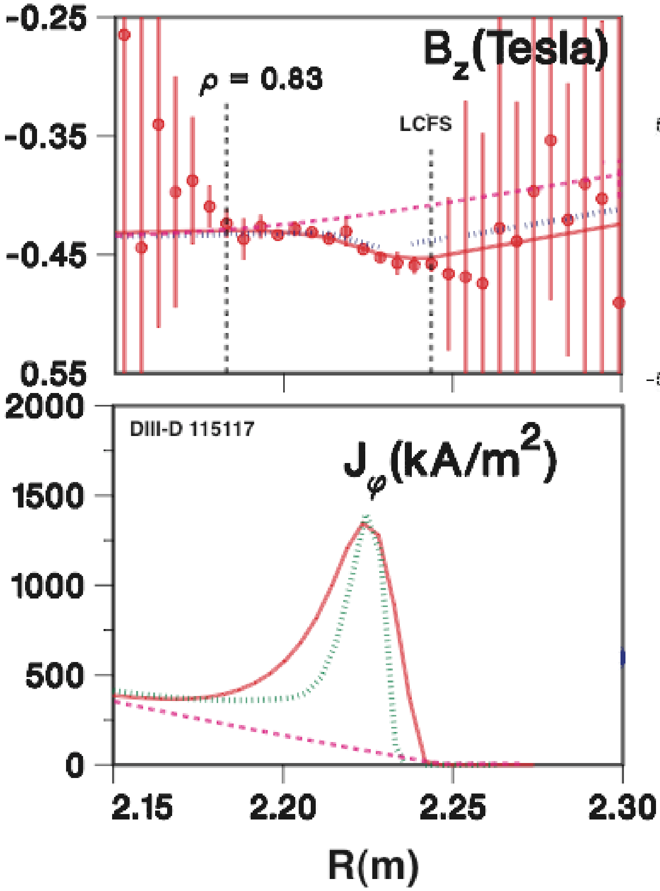

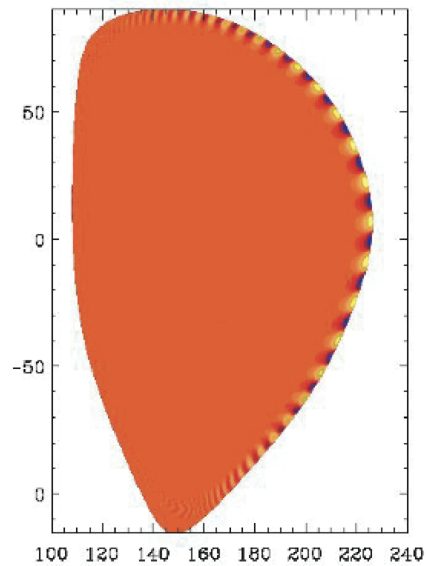

Most unstable mode is n = 25

- **EFIT equilibrium minimizes χ^2 on:**
  - **magnetics**
  - **pressure profiles**
  - **B_z(core) from MSE measurement**
  - **B_z(edge) from Li-beam measurement**
- **Implied j_{edge} peak agrees with NCLASS model**
- **CORSICA inverse solver converts this equilibrium to high radial and poloidal resolution for ELITE stability calculation**

CIII emission during ELMs shows filamentary structure consistent with n ~ 15 - 18.

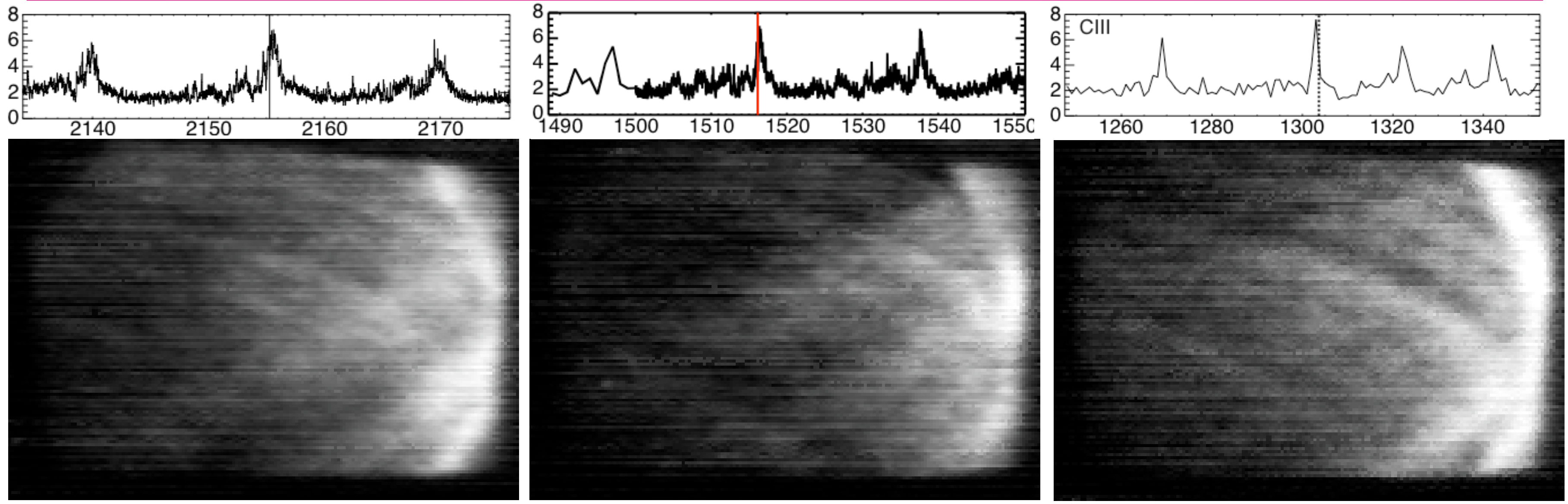

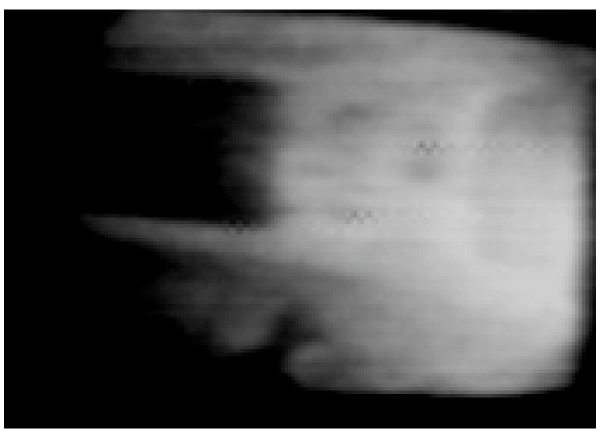

- **Gated, intensified camera views CIII (456 nm) emission tangentially at the outer midplane**
- **Images with 10 μs integration show filamentary structure at ELM crash consistent with toroidal n ~ 17; estimate q ~ 4**

ELITE stability calculation indicates most unstable modes are $14 \leq n \leq 24$; structure agrees with CIII images.

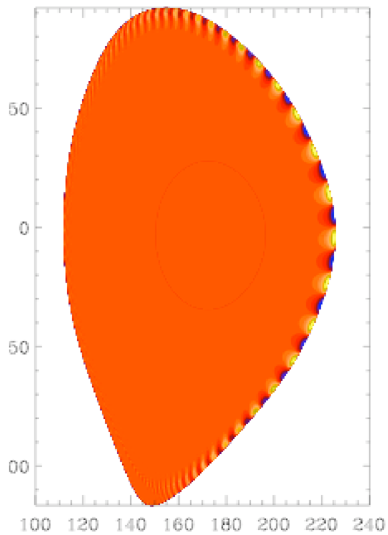

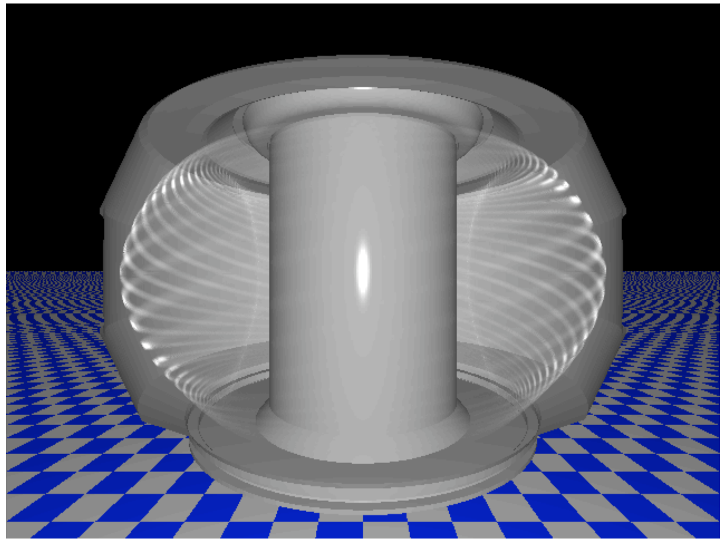

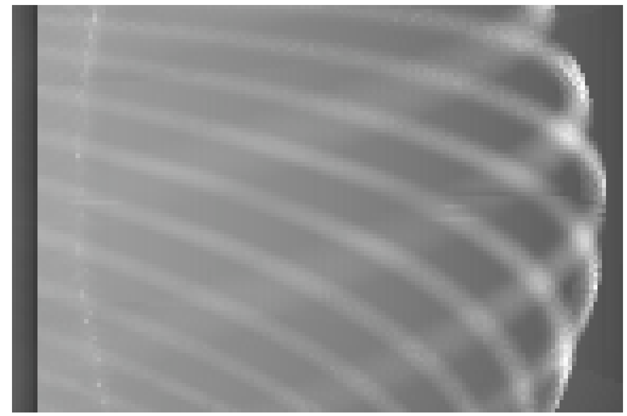

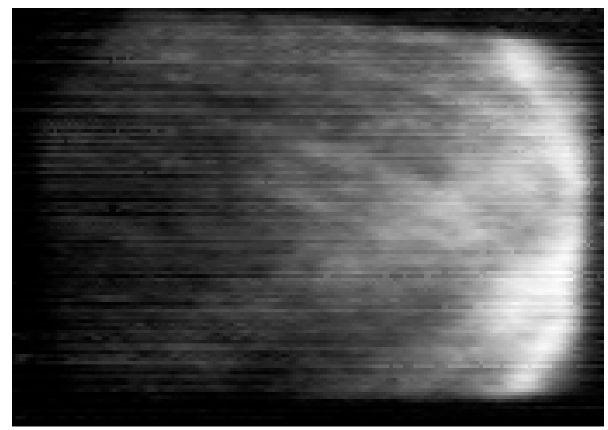

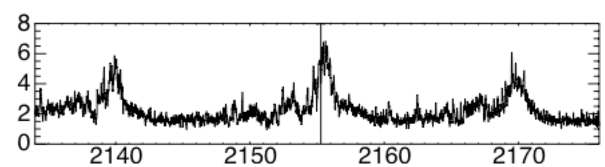

- ELITE linear P-B calculation on kinetic equilibrium shows broad maximum $14 \leq n \leq 24$ in n-spectrum of most unstable modes
- Calculated structure of n = 18 mode similar to images
  - Poloidal structure similar to outer midplane SOL structure in images
  - 3D structure has similar m/n structure seen in images

Pedestal/SOL ELM Dynamics

Large expulsion of pedestal density to far SOL at high radial velocity during ELMs

Zeng HMWS03

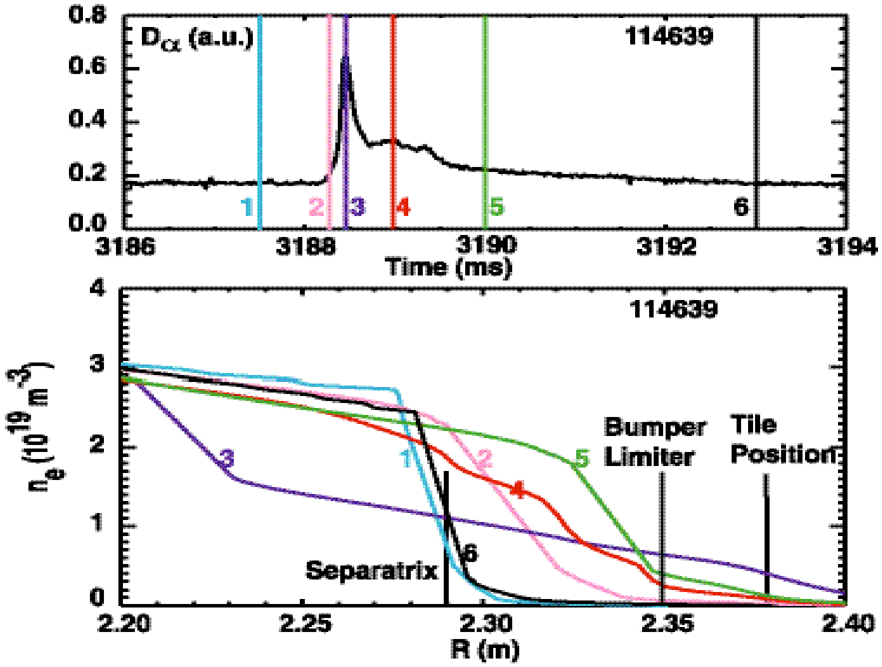

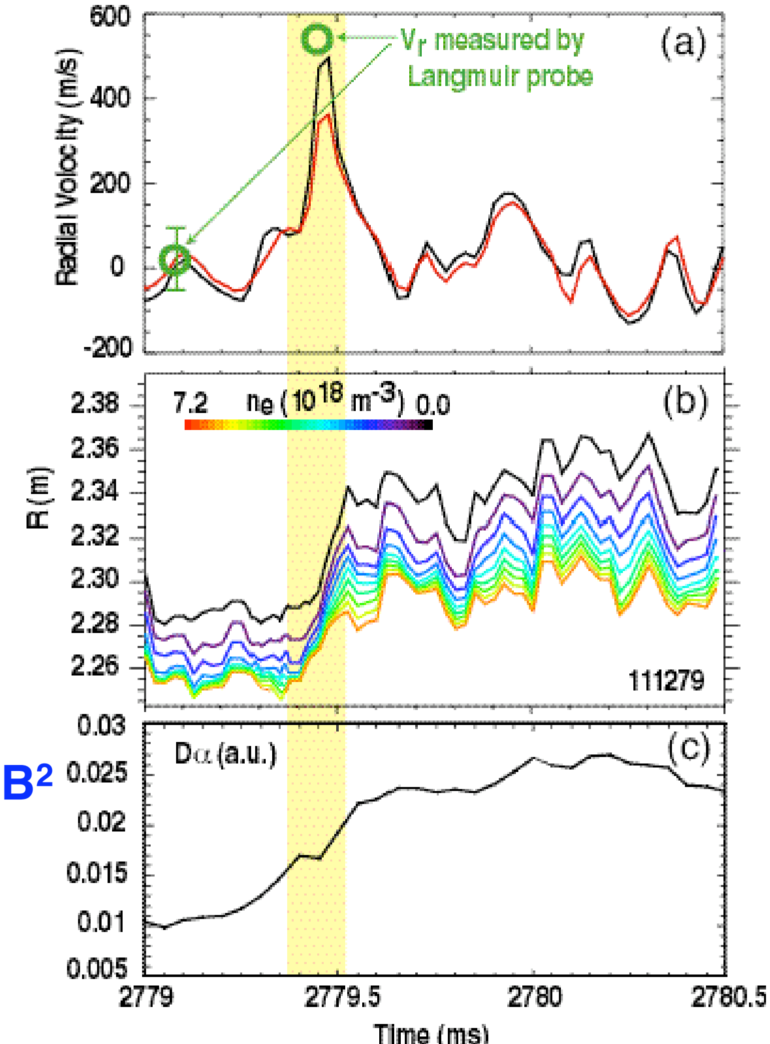

- n_e profile broadens to vessel wall
- Radial velocity in SOL, v_r ~ 0.6 km/s inferred from n_e evolution and E x B / B^2
- T_i of particles striking first wall is a critical issue for evaluation of Be wall survivability in ITER

BES data shows development of pedestal density perturbation into localized filament

McKee, Boedo EPS04

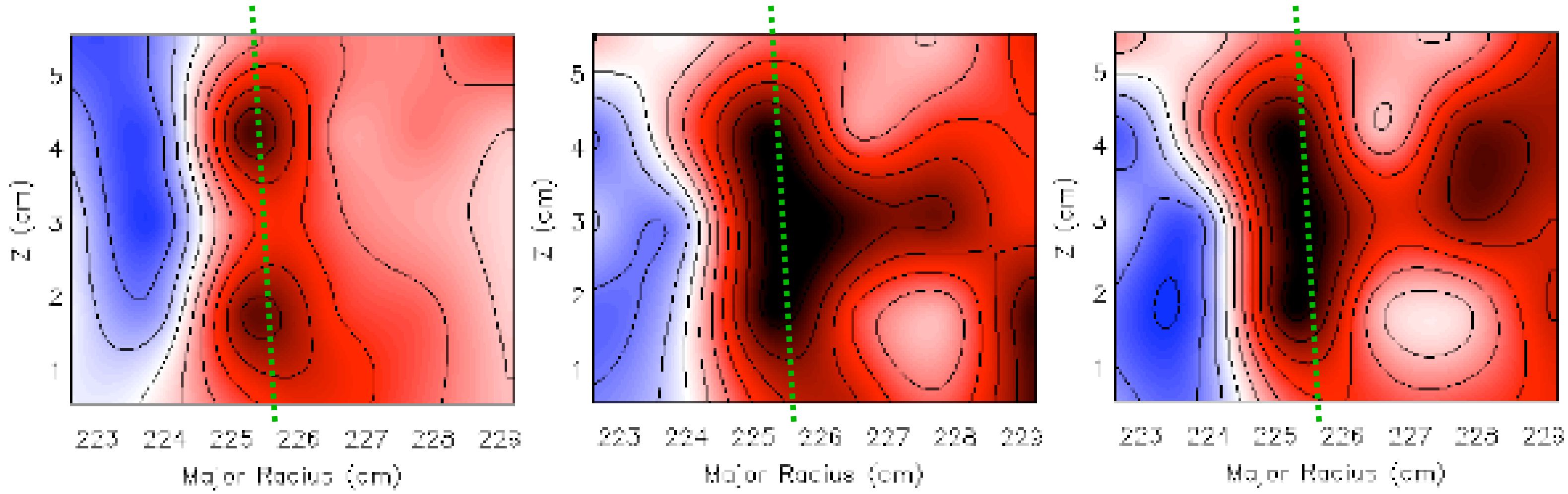

- **Density perturbation shows poloidal mode structure during linear phase**
  - **Positive perturbation (red), negative perturbation (blue), separatrix (green)**

- **Non-linear phase shows poloidally localized perturbation launched into SOL**

BOUT non-linear ELM simulations show toroidally localized "finger" bursts radially into SOL

Snyder EPS04

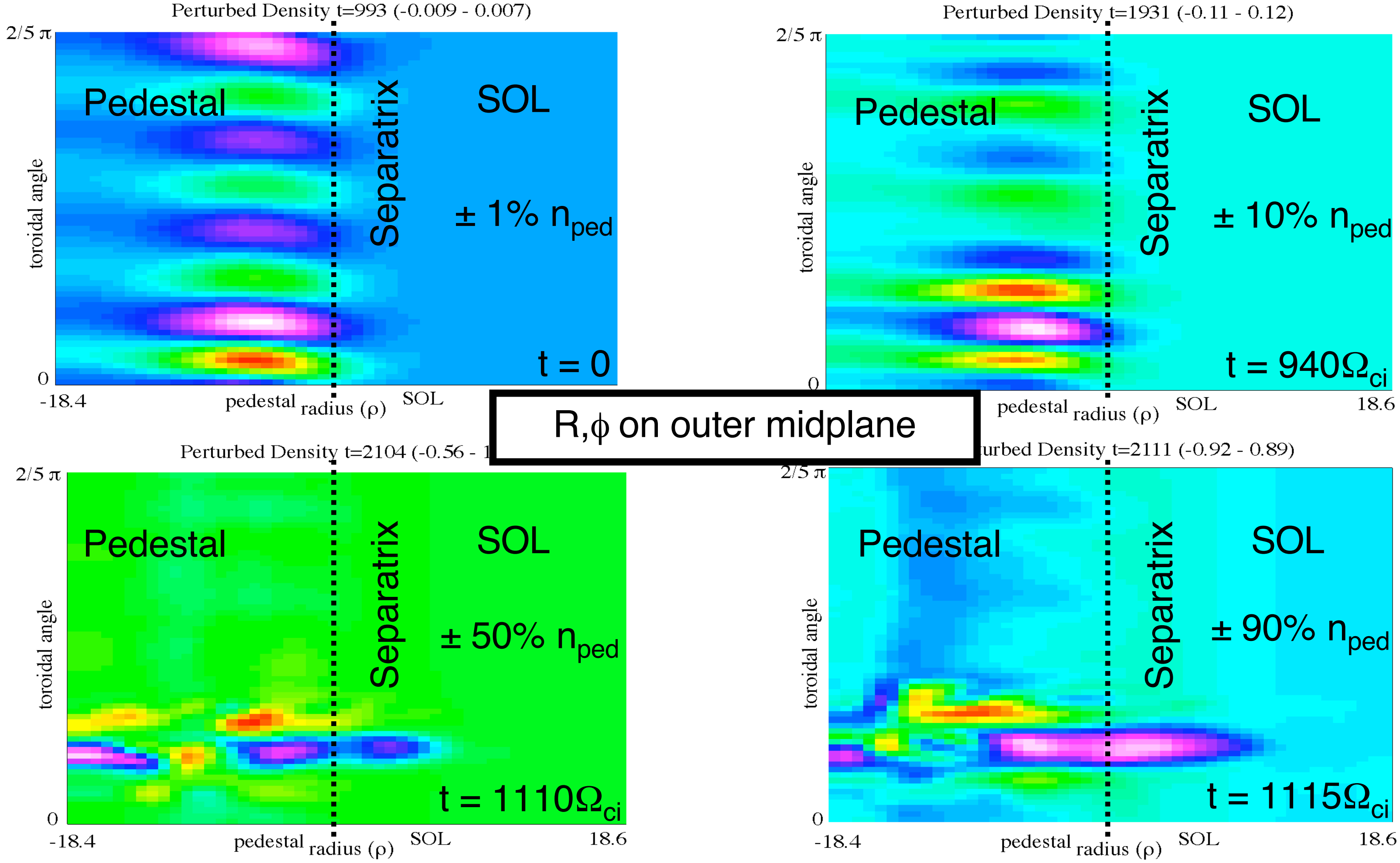

- **Burst is toroidally localized "finger" that is an extended filament along the field line.**

BOUT ELM simulation shows expected peeling-ballooning perturbation in early phase, irregular filaments later

Snyder EPS04

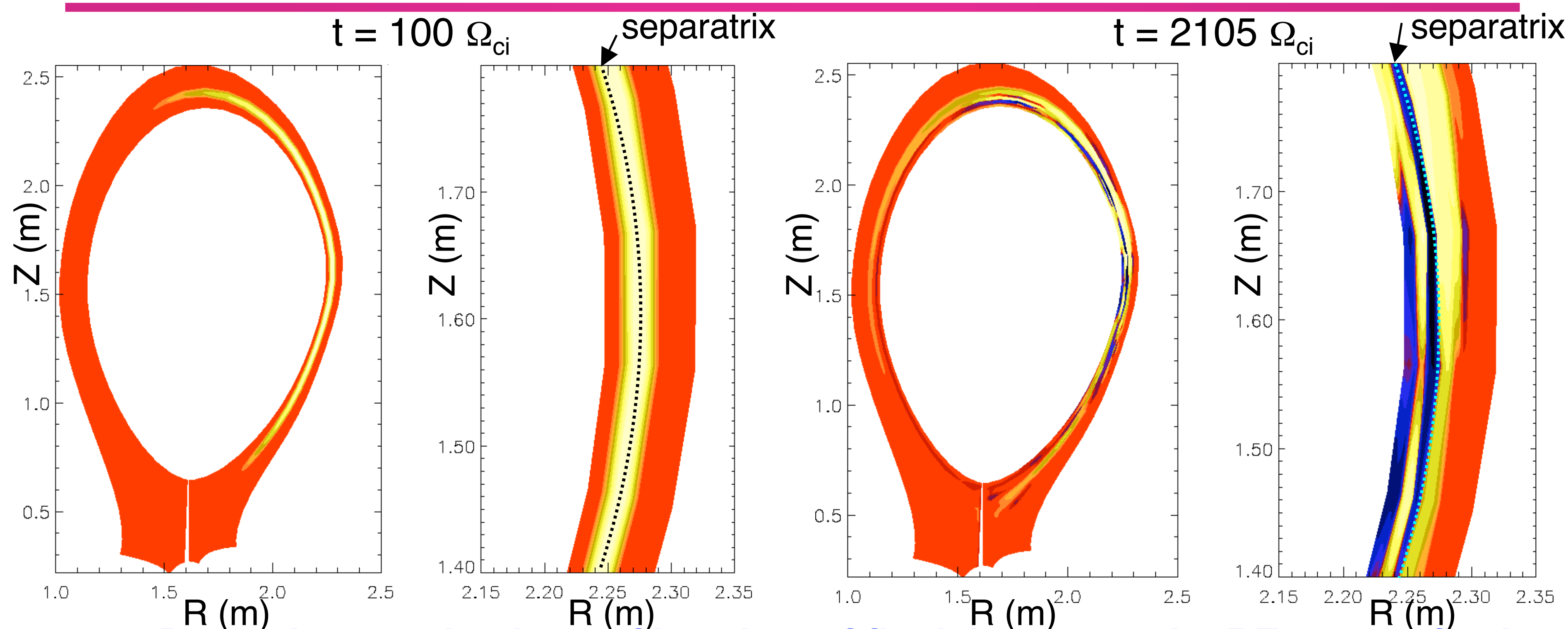

- Plots show projections of bundles of field lines onto the RZ plane - field lines extend into and out of page (radial vs parallel)
- Linear phase: Mode has expected characteristics of linear mode, radial and poloidal extent, n ~ 20, γ/ω_A~ 0.15
- Fast Burst: Filaments extended along the field, but irregular

Delay of inner vs outer D_α about 3x the difference in ion transit times from midplane to targets.

- Ion transport assumed at sound speed evaluated at pedestal Te
- Scatter increases and delay time drops to small value at very low density
  - Evidence of fast electron effects ?
  - Evidence of change in character of ELM from ballooning to peeling dominated ?

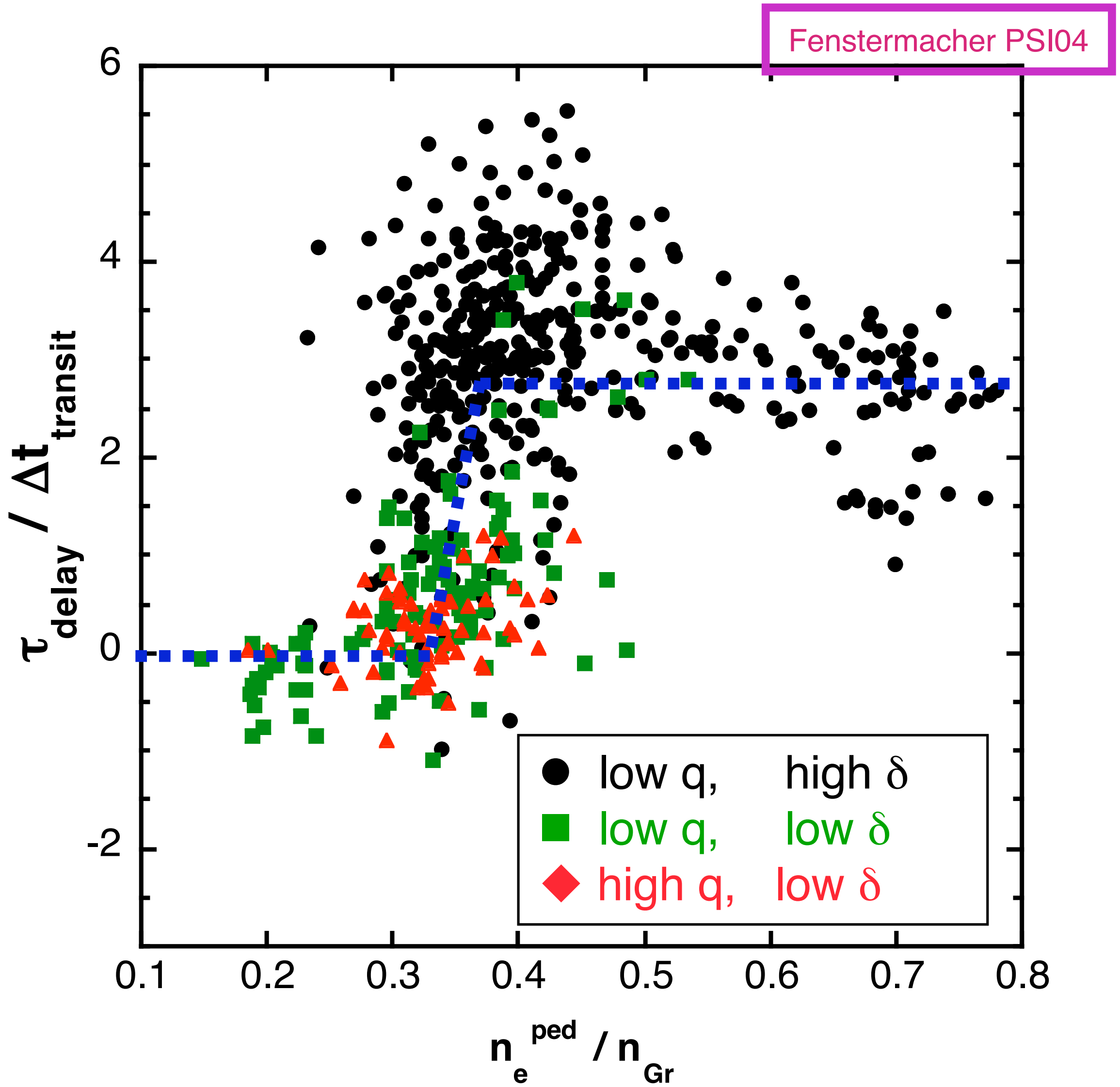

Summary and Conclusions

Favorable indications for ITER from DIII-D pedestal studies

- **Density:** Fueling techniques may allow control of $\Delta_n \propto 1 / (n_{ped} E^*)$
- **Confinement:** For small ρ_* and large minor radius in ITER:
  - $\Delta_T \propto a$ and $\Delta_T \neq f(\rho_*)$ are favorable for ITER confinement
  - $W_{ELM} / W_{ped} \sim g(\rho_*)$ favorable for ITER divertor lifetime
  - Separability of Δ_n and Δ_T may allow high pedestal and small ELMs
- **ELM-free Regime:** QH-mode a possible candidate for ITER (West EX/P3-14)
  - Successfully reproduced at DIII-D, AUG, JET, JT60-U
  - Expansion of QH-mode to ITER relevant densities in progress
- **ELM Control:** ELM suppression by stochastic edge (Evans EX2-5/Ra)
  - Expansion of ELM suppression regime to ITER-like shapes
  - Understanding suppression physics will allow coil design guidance and ELM suppression predictions for ITER

Summary

- Similarity experiment tested scaling
  - Neutral penetration physics dominates in setting density width
  - Plasma physics dominates in setting Te width (transport barrier)
  - Transport barrier not a strong function of ρ^*
  - ELM size decreased as ρ^* decreased for constant (β, ν^*, q) but neutral penetration also plays a role
- Linear P-B instability calculation in equilibrium constrained by edge poloidal field data shows unstable intermediate-n modes
  - Fast camera images show similar mode structure
  - Ampere's law calculation of j_{edge} agrees with edge $j_{bs} + j_{PF}$
- Pedestal / SOL dynamics shows evidence for rapid, filamentary behavior
  - Initial non-linear ELM simulations with BOUT show poloidal and toroidal localization
- These experiments have increased our understanding of pedestal and ELM physics

Conclusions

- **Measurements and scaling of the density pedestal width and the pressure gradient at ELM onset agree with predictive models**
  - **Neutral penetration physics dominates in setting n_e pedestal width**
  - **Linear peeling-ballooning instability physics predicts ELM onset**
- **Progress toward understanding physics that sets transport barrier width and non-linear ELM evolution**
  - **Plasma physics appears to dominate in setting Δ_T**
  - **Initial non-linear simulations show structure similar to measurements**
- **Possibility of independent control of density pedestal and temperature pedestal might allow high performance with reduced ELM energy loss**
  - **Optimize profiles to maximize pedestal pressure and minimize edge bootstrap current**
- **This represents significant progress toward predicting pedestal characteristics and ELM behavior**